

## Validation of the KC Autotuning Principle on a Multi-Tank Pilot Process

Robin De Keyser<sup>\*</sup>, Cristina I. Muresan<sup>\*\*</sup>

<sup>\*</sup>*Ghent University, DySC research group on Dynamical Systems and Control, Ghent, Belgium (e-mail: Robain.DeKeyser@UGent.be)*

<sup>\*\*</sup>*Technical University of Cluj-Napoca, Department of Automation, Cluj-Napoca, Romania  
(corresponding author, e-mail: Cristina.Muresan@aut.utcluj.ro)*

---

**Abstract:** PIDs are the most widely used controllers in industrial applications. This particular interest generates on-going research regarding simplified tuning methods appealing to the industrial user. Such methods refer also to a fast design of PID controllers in the absence of a mathematical model of the process. Autotuners represent one way of achieving such a fast design. In this paper, the experimental validation of a previously presented *direct* autotuner is presented. The autotuning method requires only one simple sine test on the process to compute the PID controller parameters. The case study consists in the Quanser Six Tanks Process. Comparisons with other popular tuning methods are also presented. The results show that the proposed autotuning method is a valuable option for controlling industrial processes.

**Keywords:** autotuning, PID control, experimental validation

---

### 1. INTRODUCTION

Although numerous advanced control strategies have shown that better closed loop results could be obtained in comparison to the PID (proportional-integrative-derivative) algorithms, the latter are still the most widely used control strategies in industrial applications (Åström and Hägglund, 2004). This is due to the simplicity of the tuning, which is of great value to the non-expert industrial user. To tune a PID controller, a mathematical model of the process may or may not be available. Frequently, in industrial applications the need for a fast tuning of PIDs implies skipping the mathematical modeling of the process. This aspect has resulted in an ongoing interest to produce better and easy-to-use autotuning techniques.

Autotuning methods can be classified in direct and indirect autotuners. Both types use a simple process test as the basis to generate the PID parameters, e.g. a step test, a relay test, a sine test. The direct methods produce the controller parameters without the need for first identifying a process model; the indirect methods first estimate a (simplified) process model, such as a first/second order plus dead-time (FOPDT/SOPDT) model. Examples of popular direct autotuners are the Ziegler-Nichols (ZN) ultimate gain tuning method (Ziegler and Nichols, 1942) and the Åström-Hägglund (AH) relay autotuner (Åström and Hägglund, 1984). Examples of popular indirect autotuners are Approximate M-constrained Integral Gain Optimisation (AMIGO) (Hägglund and Åström, 2002; Akkermans and Stan, 2002; Panagopoulos et al., 2002) and Skogestad Internal Model Control (SIMC) (Skogestad, 2003). Numerous other examples exist, as well as comparisons between various autotuning methods for several case studies (Chen and Moore, 2005; Tan and Lee, 1996; Zhang and

Yang, 2014; Souza et al., 2016). Interesting surveys can be found in (Leva et al., 2002; Yu, 2006; Liu et al., 2013; Chidambaram and Sathe, 2014). A recent experimental comparison has been presented in (Berner et al., 2018).

The Kaiser-Chiara (KC) autotuning method (De Keyser et al., 2017) used in this paper is a direct autotuner. The design is based on defining a ‘forbidden region’ that includes the -1 point in the Nyquist plane. The PID parameters are then tuned such that the loop frequency response touches the border of that forbidden region. The novelty of this paper consists in the *experimental* (practical) evaluation of the KC autotuner on a real-life nonlinear multi-tank pilot process, with comparison to the well-known AMIGO and SIMC methods. The paper is structured as follows. Section 2 introduces the principle behind the KC autotuning method. Section 3 presents a numerical example. Section 4 contains the experimental validation of the method. In both sections 3 and 4 comparisons of the KC autotuning method with the SIMC and AMIGO methods are provided. The concluding remarks are presented in Section 5.

### 2. CONCEPT OF THE KC AUTOTUNING METHOD

The KC autotuning method computes the PID controller parameters using solely the value of the process frequency response and of the frequency response slope at one specific frequency  $\bar{\omega}$ . A good choice of this test frequency is the process critical (phase crossover) frequency. The resulting PID controller is robust to gain and delay variations. The underlying principle is based on defining a ‘forbidden region’ shaped as a circle including the -1 point in the Nyquist plane (Fig. 1). The forbidden region is specified via two points: a minimum gain margin (point A, default GM=2) and a minimum phase margin (point B, default PM=45°). The PID

parameters are then computed such that the slope-difference between the loop frequency response and the circle border is minimum:

$$\min_{\alpha} \left\| \left. \frac{d \operatorname{Im}}{d \operatorname{Re}} \right|_{\alpha} - \left. \frac{d \Im_L}{d \Re_L} \right|_{\omega=\bar{\omega}} \right\|, 0 \leq \alpha \leq \alpha_{\max} \quad (1)$$

where  $\left. \frac{d \Im_L}{d \Re_L} \right|_{\omega=\bar{\omega}}$  is the slope of the loop frequency response at  $\bar{\omega}$  in the Nyquist plane and  $\left. \frac{d \operatorname{Im}}{d \operatorname{Re}} \right|_{\alpha}$  is the slope of the forbidden region border as a function of the angle  $\alpha$ . The minimization problem in (1) is simply solved by computing the slope-difference for every  $\alpha$  in the range 0 to  $\alpha_{\max}=90^\circ$  (e.g. in  $1^\circ$  steps). Consider the slope of the loop frequency response  $L(j\omega) = P(j\omega)C(j\omega)$ :

$$\left. \frac{dL(j\omega)}{d\omega} \right|_{\omega=\bar{\omega}} = P(j\bar{\omega}) \left. \frac{dC(j\omega)}{d\omega} \right|_{\omega=\bar{\omega}} + C(j\bar{\omega}) \left. \frac{dP(j\omega)}{d\omega} \right|_{\omega=\bar{\omega}} \quad (2)$$

where  $C(j\bar{\omega})$  and  $P(j\bar{\omega})$  are the controller and process frequency responses at the test frequency  $\bar{\omega}$ . The process frequency response  $P(j\bar{\omega})$  and the process frequency response slope  $\left. \frac{dP(j\omega)}{d\omega} \right|_{\omega=\bar{\omega}}$  are determined based on a single sine test (De Keyser et al., 2016; De Keyser et al., 2019). For each  $\alpha$ , the loop frequency response point  $L(j\bar{\omega})$  can be easily computed as the complex number corresponding to the point on the KC circle:

$$C(j\bar{\omega}) = \frac{L(j\bar{\omega})}{P(j\bar{\omega})} = a \left( 1 + j \frac{b}{a} \right) \quad (3)$$

Then (3) allows to calculate the parameters of the PID as:

$$C(s) = k_p \left[ 1 + \frac{1}{T_i s} + T_d s \right] \quad (4)$$

with  $k_p$  the proportional gain,  $T_i$  and  $T_d$  the integral and derivative time constants, with  $T_i = r T_d$  ( $r$  can be further optimized, but in the experiments of section 4 it is by default taken  $r=4$ , as also suggested in (Åström and Hägglund, 2004)). Then replacing (4) into (3) allows for the computation of the PID parameters:

$$k_p = a, T_i = \frac{2}{a\bar{\omega}} \left( b + \sqrt{b^2 + a^2} \right) \text{ and } T_d = \frac{T_i}{4} \quad (5)$$

Once  $C(s)$  is known,  $\left. \frac{dC(j\omega)}{d\omega} \right|_{\omega=\bar{\omega}}$  can easily be calculated in a numerical way. The right-hand side of (2) is then completely known and the slope of the loop frequency response can be written as the sum of its real  $\Re_L$  and imaginary  $\Im_L$  parts as:

$$\left. \frac{dL(j\omega)}{d\omega} \right|_{\omega=\bar{\omega}} = \left. \frac{d \Re_L}{d\omega} \right|_{\omega=\bar{\omega}} + j \left. \frac{d \Im_L}{d\omega} \right|_{\omega=\bar{\omega}} \quad (6)$$

Using (6), the slope of the loop frequency response in the Nyquist plane can be computed as the ratio:  $\left. \frac{d \Im_L}{d \Re_L} \right|_{\omega=\bar{\omega}}$ .

To compute the slope of the KC circle, trigonometric relations are used in Fig. 1. A point on the circle is defined by its real and imaginary parts:

$$\operatorname{Re}(\alpha) = -C + R \cdot \cos(\alpha) \quad (7)$$

$$\operatorname{Im}(\alpha) = -R \cdot \sin(\alpha) \quad (8)$$

**Table 1. PID controller parameters for the SIMC, AMIGO and ZIEGLER-NICHOLS methods**

Process model	SIMC method (series PID)		
$\frac{k}{(T_1 s + 1)(T_2 s + 1)} e^{-\tau s}$ $T_1 > T_2$	$k_{p\_series} = \frac{T_1}{k(T_c + \tau)}$ $T_c = \tau$	$T_{i\_series} = \min(T_1, 4 \cdot (T_c + \tau))$	$T_{d\_series} = T_2$
$\frac{k}{s(Ts + 1)} e^{-\tau s}$	$k_{p\_series} = \frac{1}{k(T_c + \tau)}$ $T_c = \tau$	$T_{i\_series} = 4 \cdot (T_c + \tau)$	$T_{d\_series} = T$
AMIGO method			
$\frac{k}{Ts + 1} e^{-\tau s}$	$k_p = \frac{1}{k} \left( 0.2 + 0.45 \frac{T}{\tau} \right)$	$T_i = \frac{0.4\tau + 0.8T}{\tau + 0.1T} \tau$	$T_d = \frac{0.5\tau T}{0.3\tau + T}$
$\frac{k_v}{s} e^{-\tau s}$	$k_p = \frac{0.45}{k_v}$	$T_i = 8\tau$	$T_d = 0.5\tau$
Ziegler-Nichols ultimate gain method (ZN-UG)			
$k_{cr}$ – critical gain, $T_{cr}$ – period of oscillations	$k_p = 0.6 k_{cr}$	$T_i = \frac{T_{cr}}{2}$	$T_d = \frac{T_{cr}}{8}$

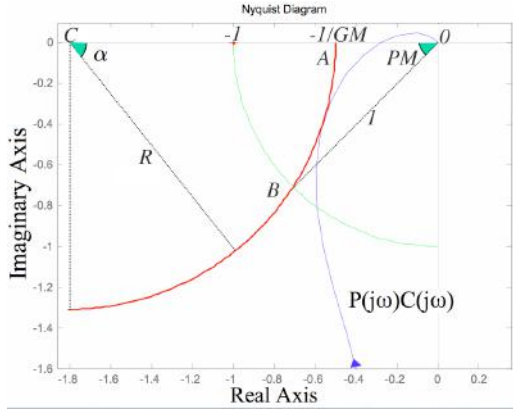


Fig. 1. The loop frequency response (blue line) and the ‘forbidden region’ (the KC circle, red line).

The slope of the forbidden region border is then:

$$\left. \frac{d \operatorname{Im}}{d \operatorname{Re}} \right|_{\alpha} = -\frac{\operatorname{Re}(\alpha) + C}{\operatorname{Im}(\alpha)} = \frac{\cos(\alpha)}{\sin(\alpha)} \quad (9)$$

### 3. A NUMERICAL EXAMPLE

The KC tuner has been validated on a numerous number of simulated benchmark systems (De Keyser et al., 2017). One more example is given here:

$$P(s) = \frac{1}{s(s+1)} e^{-s} \quad (10)$$

The PID controller parameters computed using the KC method, as well as using the SIMC, ZN-UG and AMIGO methods are given in Table 2. The step tracking and load disturbance rejection results are shown in Figs. 2a) and b). It is clear that the proposed method offers good closed loop results.

**Table 2. PID Controller Parameters For The Numerical Example**

	$k_p$	$T_i$	$T_d$
Proposed method	0.65	6.06	1.09
AMIGO method	0.45	16.0	1.00
SIMC method (parallel form)	0.5625	9.00	0.89
ZN-UG method	0.68	3.65	0.91

To tune the controller using the AMIGO method, the transfer function in (10) has been approximated using the Matlab identification toolbox based on the minimization of the integral of the squared error between the original and approximated transfer functions step responses:

$$P'(s) = \frac{1}{s} e^{-2s} \quad (11)$$

Figure 3 shows the Nyquist plot of the loop transfer function with the PID controller designed according to the KC tuner. This demonstrates that the design constraints have been met, the difference between the slope of the KC circle and the slope of the loop frequency response being minimum.

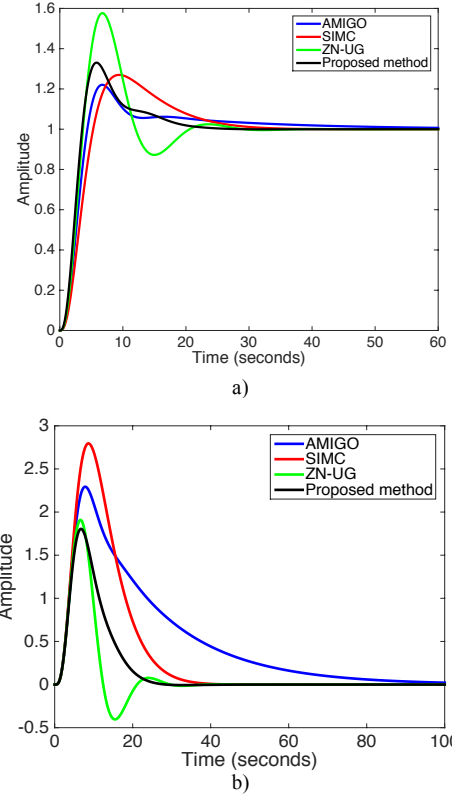


Fig. 2. a) Step reference tracking b) load disturbance rejection

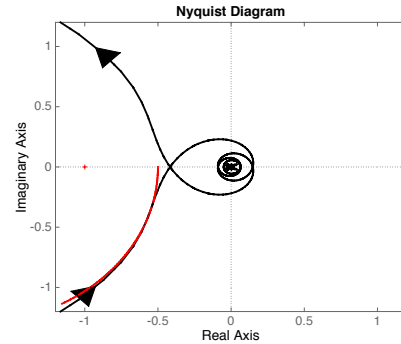


Fig. 3. Nyquist plot for the numerical example using the proposed tuning rules (black) and the “forbidden region” (red)

## 4. EXPERIMENTAL VALIDATION

### 4.1 The test process

The case study used to validate experimentally the KC autotuning method is the Quanser six tanks process given in Fig. 4. The configuration of the six tanks process is given in Fig. 5, with  $L_i$ ,  $i=1\dots 6$  denoting the level in each of the six tanks,  $V_{pj}$ ,  $j=1\dots 3$  denoting the voltages of the three pumps and  $V$  denoting the valve. As indicated in Fig. 6, the input to this high-order nonlinear process is the setpoint  $S_1$  for a P-

controller on level  $L_1$ , ref. eq. (12). The output is  $L_6$ , while the disturbance is induced by the opening/closing of valve  $V$ . The voltages supplied to the pumps are:

$$V_{p1} = 5.5 + k_{p1}(S_1 - L_1) \quad (12)$$

$$V_{p2} = k_{p2}L_2 \quad (13)$$

$$V_{p3} = k_{p3}L_3 \quad (14)$$

where  $k_{p1}=1$  (the gain of a proportional controller with setpoint  $S_1$ ) and  $k_{p2}=k_{p3}=0.5$ . The process contains a feedback loop. However, this is an 'internal' feedback loop. Its feedback signal is the level of tank 1,  $L_1$ , as indicated in (12). The feedback signal for the process-of-interest (for which the PIDs have to be tuned) is the level of tank 6 ( $L_6$ ; Fig. 6). It concerns the master loop of a master-slave (cascade) configuration.



Fig. 4. Overview of the Quanser six tanks process

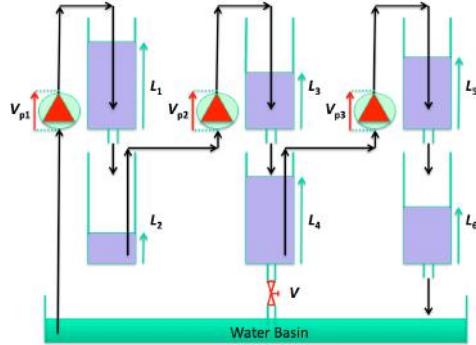


Fig. 5. Configuration of the six tanks process

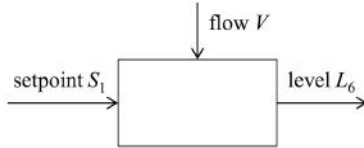


Fig. 6. Input-output model of the 6 tanks process

#### 4.2 Step test

To compute the PID parameters according to the SIMC and AMIGO methods, a sequence of four step tests has been performed on the process around the operating point 10 (initially  $S_1=10$ , then: at  $t=300 \rightarrow S_1=11$ ; at  $t=600 \rightarrow S_1=10$ ; at  $t=900 \rightarrow S_1=9$ ; at  $t=1200 \rightarrow S_1=10$ ). The resulting level measurements are shown in Fig 7a. The averaged step response of  $L_6$  is given in Fig. 7b. Using the Matlab Identification Toolbox, two simplified models have been identified based on this averaged stepresponse: a FOPDT  $P_1(s)$  transfer function and a SOPDT  $P_2(s)$  transfer function:

$$P_1(s) = \frac{0.82}{1+38s} e^{-30s} \quad (15)$$

$$P_2(s) = \frac{0.82}{(1+24s)(1+23s)} e^{-22s} \quad (16)$$

The comparative step responses of these models and the experimental data are included in Fig. 8, showing good approximation accuracy.

Computing the PID parameters for the SIMC and AMIGO methods according to Table 1 and using the models in (15) and (16), the following results have been obtained:

$$C_{SIMC\_series}(s) = 0.67(1 + \frac{1}{24s})(1+23s) \text{ or in its parallel form,}$$

$$C_{SIMC}(s) = 1.312(1 + \frac{1}{47s} + 11.744s) \quad (17)$$

$$C_{AMIGO}(s) = 0.94(1 + \frac{1}{38s} + 12s) \quad (18)$$

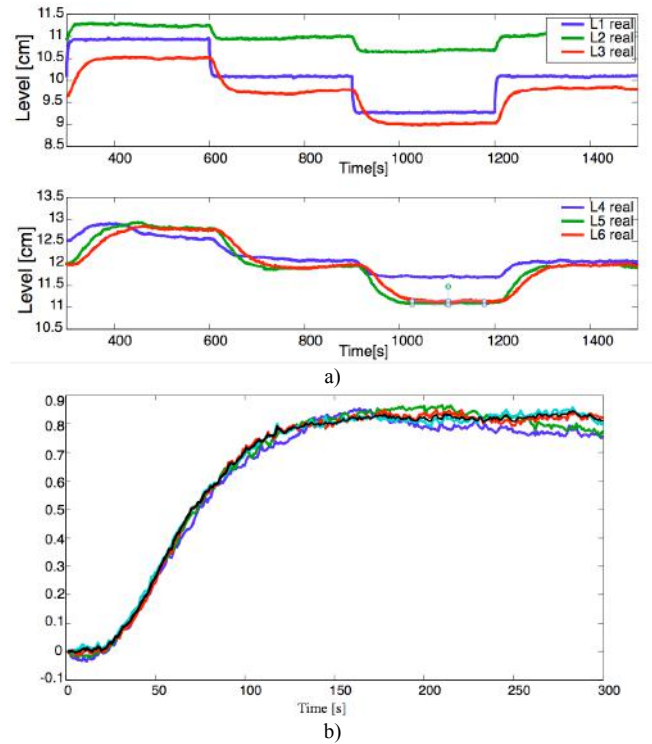


Fig. 7. a) Step tests, b) Averaged step response on  $L_6$

#### 4.3 Sine test

To compute the PID parameters using the KC autotuning method, the process frequency response and the process frequency response slope are computed from the response of a single sine test experiment:

$$S_1(t) = 10 + \sin\left(\frac{2\pi}{120}t\right) \quad (19)$$

with the test frequency  $\bar{\omega} = \frac{2\pi}{120}$  being around the process critical frequency (phase crossover frequency). Fig. 9a)

shows the input  $S_1$  and the output  $L_6$ , while Fig. 9b) shows the steady state ( $Y_{ss}$ ) and transient ( $Y_{tr}$ ) signals extracted from  $L_6$ .

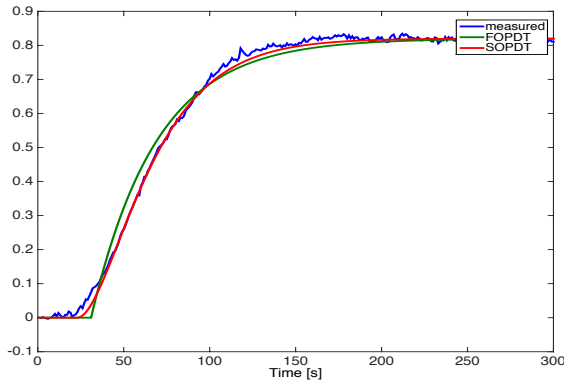


Fig. 8. Comparative step response of the two models and experimental data for output  $L_6$

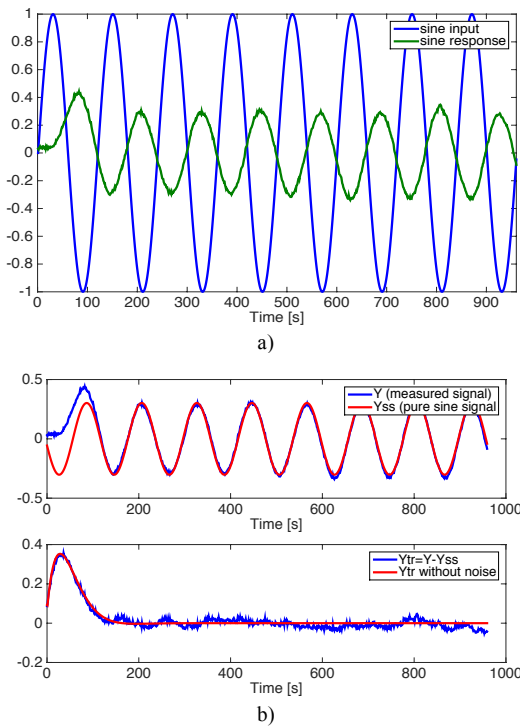


Fig. 9. a) Experimental results for the sine test – output  $L_6$ ; b) Steady state and transient components of  $L_6$

These signals are then used in the computation of the process frequency response and its slope (De Keyser et al., 2016; De Keyser et al., 2019):

$$P(j\bar{\omega}) = -0.297 - 0.0565j \quad (20)$$

$$\left. \frac{dP(j\omega)}{d\omega} \right|_{\omega=\bar{\omega}} = 6.12 + 14.9j \quad (21)$$

Using the algorithm of Section 2, the PID controller is then:

$$C_{KC}(s) = 1.5 \left( 1 + \frac{1}{54s} + 14s \right) \quad (22)$$

Fig. 10 shows the Nyquist plane with the loop frequency response in black touching the ‘forbidden region’ KC circle in red.

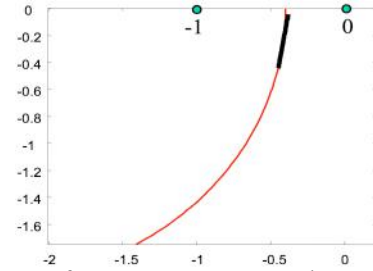


Fig. 10. Loop frequency response at the test frequency (black) and KC circle (red)

#### 4.4 Nominal PID tests

The experimental results considering the KC, SIMC and AMIGO controllers are given in Figs. 11a) – d). The first event (Fig. 11a) consists of a setpoint change from 12cm to 10cm, thus around the nominal operating point used in the step and sine tests. The second event (Fig. 11b) presents the closed loop behavior after an important disturbance caused by opening the valve V (ref. Fig. 5). The next event (Fig. 11c) consists of another important disturbance by closing the valve 5.

#### 4.5 Robustness test

The multiple-tank process is quite nonlinear, due to the square-root relationship between pressure and flow in each tank. Based on the concept of local linearization, the PID tuning will be optimal around the operating point. This means: in the range where the tuning experiment has been executed. In the KC-tuner, this experiment is a sine-test around a selected operating point. In the multiple-tank process experiment the operating point has been selected as: output (level) about 10cm. In order to validate the controller performance at other operating points of this highly nonlinear process, a robustness test has been performed (Fig. 11d). This test has been done at a far-away operating point: output (level) about 20cm and it consists of a setpoint change from 22cm to 20cm. In all cases Figs. 11a) - d), the KC autotuner performs equally well - if not better - compared to the other tuning approaches. Moreover it has the advantage that it is a *direct* autotuner: no FOPDT/SOPDT model has to be identified.

## 5. CONCLUSIONS

As PIDs still dominate the world of industrial control engineering, it is natural to continue with the development of novel techniques for easier tuning by practitioners. Successful autotuning methods assume a simple process test, which directly leads to a set of useful PID parameters. Mathematical modeling and identification requires too much skills and it is time consuming. These ideas have been the basis for the development of the KC autotuner. In this paper the experimental validation of this method is presented. Apart from the case study (Quanser six tanks process), a numerical example is also provided. Comparisons with other popular tuning methods are presented. The numerical as well as the

experimental results show that the KC autotuning method is an excellent option for tuning industrial controllers, especially since the resulting PID exhibits good robustness (which is a direct result of the tuning concept itself).

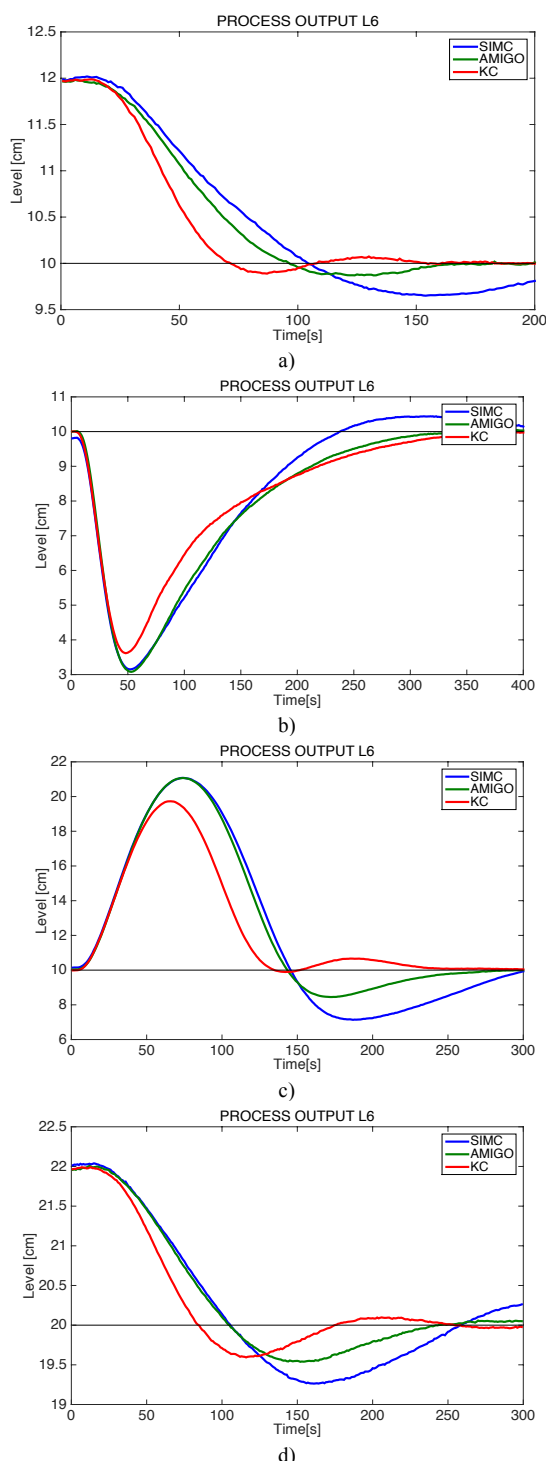


Fig.11. a) Closed loop setpoint tracking b) Disturbance rejection opening valve c) Disturbance rejection closing valve d) Robustness validation

#### ACKNOWLEDGEMENT

Cristina I. Muresan is financed by a grant of the Romanian National Authority for Scientific Research and Innovation,

CNCS/CCCDI-UEFISCDI, project number PN-III-P1-1.1-TE-2016-1396, TE 65/2018.

#### REFERENCES

- Åström, K.J., Hägglund, T. (2004). Revisiting the Ziegler–Nichols step response method for PID control. *J. Process. Contr.*, vol. 14, pp. 635–650.
- Ziegler, J.G., Nichols, N.B. (1942). Optimum settings for automatic controllers. *Trans ASME*, vol. 64, pp. 759–768.
- Hägglund, T., Åström, K.J. (2002). Revisiting the Ziegler–Nichols tuning rules for PI control. *Asian Journal of Control*, vol. 4, pp. 364–380.
- Akkermans, S.G., Stan, S.G. (2002). Digital servo IC for optical disc drives. *Control Engineering Practice*, vol. 9, pp. 1245–1253.
- Panagopoulos, H., Åström, K.J. and Hägglund, T. (2002). Design of PID controllers based on constrained optimisation, *IEEE Proceedings—Control Theory and Applications*, vol. 149, pp. 32–40.
- Skogestad, S. (2003). Simple analytic rules for model reduction and PID controller tuning. *J. Process. Contr.*, vol. 13, pp. 291–309.
- Chen, Y.Q., Moore, K.L. (2005). Relay feedback tuning of robust PID controllers with iso-damping property. *Trans. Syst. Man. Cybern.*, vol. 35, pp. 23–31.
- Åström, K.J., Hägglund, T. (1984). Automatic tuning of simple regulators with specifications on phase and amplitude margins. *Automatica*, vol. 20, pp. 645–651.
- Tan, K.K., Lee, T.H. and Wang, Q.G. (1996). Enhanced automatic tuning procedure for process control of PI/PID controllers. *AIChE J.*, vol. 42, pp. 2555–2562.
- Zhang, W., Yang, M. (2014). Comparison of auto-tuning methods of PID controllers based on models and closed-loop data. *Proc. of the 33rd Chinese Control Conference*, DOI: 10.1109/ChiCC.2014.6895548.
- De Souza, M.R.S.B., Murofushi, R.H., De Souza Tavares, J. J.-P.Z. and Ribeiro, J.F. (2016). Comparison Among Experimental PID Auto Tuning Methods for a Self-balancing Robot. In: Santos Osório, F., Sales Gonçalves, R. (eds) *Robotics*, pp. 72–86. Springer, Cham.
- Leva, A., Cox, C. and Ruano, A. (2002). Hands-on Pid autotuning: a guide to better utilization. *IFAC Professional Brief*
- Yu, C.C. (2006). *Autotuning of PID controllers - A relay feedback approach*. Springer-Verlag Ltd, London.
- Liu, T., Wang, Q.G. and Huang, H.P. (2013). A tutorial review on process identification from step or relay feedback test, *Journal of Process Control*, vol. 23, pp. 1597–1623.
- Chidambaram, M., Sathe, V. (2014). *Relay autotuning for identification and control*. Cambridge University Press, Cambridge.
- Berner, J., Soltesz, K., Hägglund, T. and Åström, K.J. (2018). An experimental comparison of PID autotuners. *Control Engineering Practice*, vol. 73, pp. 124–133.
- De Keyser, R., Ionescu, C.M. and Muresan, C.I. (2017). Comparative Evaluation of a Novel Principle for PID Autotuning. *Proc. of the Asian Control Conference*, DOI:10.1109/ASCC.2017.8287335, pp. 1164–1169.
- De Keyser, R., Muresan, C.I. and Ionescu, C.M. (2016). A Novel Auto-tuning Method for Fractional Order PI/PD Controllers. *ISA Transactions*, vol. 62, pp. 268–275.
- De Keyser, R., Muresan, C.I. and Ionescu, C.M. (2019). A single sine test can robustly estimate a system's frequency response slope. *International Journal of Systems Science*, under review.